



# Structural relaxation in AgPO<sub>3</sub> glass followed by *in situ* ionic conductivity measurements



C.B. Bragatto<sup>a,\*</sup>, D.R. Cassar<sup>a</sup>, O. Peitl<sup>a</sup>, J.-L. Souquet<sup>b</sup>, A.C.M. Rodrigues<sup>a,\*</sup>

<sup>a</sup> Laboratório de Materiais Vítreos (LaMaV), Universidade Federal de São Carlos, São Carlos, (UFSCar), Brazil

<sup>b</sup> Laboratoire d'Electrochimie et de Physicochimie des Matériaux et des Interfaces, (LEPMI) Grenoble-INP, Saint Martin d'Hères Cedex, France

## ARTICLE INFO

### Article history:

Received 11 November 2015

Received in revised form 14 January 2016

Accepted 18 January 2016

Available online xxxx

### Keywords:

Structural relaxation

Ionic conductivity

Kohlrausch exponent

Impedance spectroscopy

Viscosity

## ABSTRACT

The structural relaxation kinetics of a silver meta-phosphate glass (AgPO<sub>3</sub>) is investigated using a method based on the isothermal variation of its ionic conductivity over time. Samples of AgPO<sub>3</sub> glass from the same batch were pre-annealed at 433 K or 418 K and then relaxed at different temperatures within this temperature range, which is close to its glass transition temperature measured by differential scanning calorimetry,  $T_g^{DSC} = 438$  K. Ionic conductivity data were continuously collected by impedance spectroscopy during the isothermal relaxation process. The variation of the electrical conductivity over time is well described by the Kohlrausch expression ( $\Phi(t) = \exp[-(t/\tau_0^K)^\beta]$ ), in which  $\tau_0^K$  is the characteristic relaxation time and  $\beta$  a stretch exponent. Different values of  $\beta$  were found when the glass structure expanded or contracted during relaxation. In addition, viscosity values calculated by the Maxwell relationship using  $\langle \tau \rangle$  from conductivity data and a shear modulus taken from the literature are in accordance with the experimental viscosity measured in the same temperature range, thus validating the use of ionic conductivity to unveil glass structural relaxation.

© 2016 Elsevier B.V. All rights reserved.

## 1. Introduction

Since glasses are out of thermodynamic equilibrium, their physical properties do not depend solely on the traditional thermodynamic variables such as pressure and temperature. Hence, at least one additional parameter is needed to define the degree of structural disorder of the frozen liquid. This additional parameter is the so-called fictive temperature ( $T_f$ ). At this temperature, both the glass and metastable supercooled liquid would have the same structure.

When a glass is annealed long enough at a given temperature  $T_{(1)}$  it reaches an equilibrium structure corresponding to that of the metastable liquid phase at this temperature. In this case, the fictive temperature of this material is  $T_{f(1)} = T_{(1)}$ . However, it is possible to change the fictive temperature if a new equilibrium state is reached at a different temperature  $T_{f(2)}$ . The structural change towards a new equilibrium state is called *structural relaxation*. During this structural relaxation process, all the properties that depend on the structure change over time.

Eq. (1) expresses the rate of an isothermal change for a given property during relaxation [1]:

$$\left(\frac{\partial P}{\partial t}\right)_{T,P} = -\frac{(P_t - P_\infty)}{\tau_P} \quad (1)$$

In this equation,  $P_t$  is the value of a property  $P$  at a time  $t$ ,  $P_\infty$  is the value of  $P$  when equilibrium is reached, and  $\tau_P$  is the relaxation time related to the investigated property. If  $\tau_P$  is considered constant, and defining  $P_0$  as the value of  $P$  at  $t = 0$ , the integration of (1) leads to the following relation:

$$\frac{P_t - P_\infty}{P_0 - P_\infty} = \Phi = \exp\left[-\left(\frac{t}{\tau_P}\right)\right], \quad (2)$$

where  $\Phi$  is the relaxation function, which is equal to zero when equilibrium is reached.

Note that if several parallel relaxation processes are possible, each having a specific relaxation time  $\tau_P$ ,  $\Phi$  may be expressed by the Kohlrausch [2] expression, which is also known as the stretched exponential equation:

$$\Phi = \exp\left[-\left(\frac{t}{\tau_P^K}\right)^\beta\right], \quad (3)$$

where  $0 < \beta \leq 1$ , and  $\tau_P^K$  is a characteristic relaxation time. The exponent  $\beta$  can be interpreted as a coefficient corresponding to a distribution of the relaxation time spectrum [3]. Note that if all the characteristic properties (i.e., density, refractive index, conductivity...) are proportional to each other—which would be the case in a limited temperature range—this should lead to the same relaxation time, regardless of the property under study.

\* Corresponding authors.

E-mail addresses: [caio.bragatto@gmail.com](mailto:caio.bragatto@gmail.com) (C.B. Bragatto), [acmr@ufscar.br](mailto:acmr@ufscar.br) (A.C.M. Rodrigues).

In this work, the studied property ( $P$ ) is ionic conductivity ( $\sigma$ ) and the chosen glass is  $\text{AgPO}_3$ , whose glass transition temperature is low,  $T_g^{\text{DSC}} = 438$  K, and whose ionic transport is due to  $\text{Ag}^+$  cations [4]. Electrical conductivity measurements have been carried out to follow *in situ* the kinetics of the structural relaxation of an  $\text{AgPO}_3$  glass. This technique allows one to obtain a large number of experimental data during the relaxation process, and consequently, well defined isothermal relaxation curves. However, this is not the case when the relaxation kinetics is determined based on the classical measurements of properties such as density [5,6] or refractive index [7] which are measured not continuously over time.

Therefore, the structural relaxation time  $\tau_{\sigma}^K$  will be estimated in the temperature range of 418 to 433 K from variations in isothermal conductivity over time. Structural relaxation has already been detected using *in situ* complex impedance measurements in a window glass [8]. In addition, ionic conductivity has been applied to monitor structural relaxation in glassy pharmaceutical products [9] and also in the CKN glass [10].

As a consistency test, viscosity will be calculated using relaxation time from ionic conductivity and a shear modulus from the literature, both linked by the Maxwell fluid equation,

$$\eta = G\langle\tau\rangle, \quad (4)$$

where the average relaxation time,  $\langle\tau\rangle$  is expressed by [1].

$$\langle\tau\rangle = \frac{\tau_p^K}{\beta} \Gamma\left(\frac{1}{\beta}\right). \quad (5)$$

Thus, calculated values of viscosity will be compared with experimental viscosity data obtained in the same temperature range for the same batch of glassy  $\text{AgPO}_3$ . A discussion on the variation of  $\beta$  parameter is proposed.

## 2. Materials and methods

Glasses were prepared by melting and quenching an equimolar mixture of  $\text{AgNO}_3$  and  $\text{NH}_4\text{H}_2\text{PO}_4$  powders with purity over 99.5% from Sigma Aldrich. After 1 h of melting at 723 K in a borosilicate crucible (Pyrex®), drops of melt were splat-quenched at room temperature between two stainless steel plates. Several flat disk-shaped samples of transparent  $\text{AgPO}_3$  glass with an average diameter of 8 mm and thickness of 1 mm were obtained from the same batch. The glass transition temperature ( $T_g^{\text{DSC}} = 438$  K) was measured by differential scanning calorimetry at a heating rate of  $10 \text{ K min}^{-1}$  (DSC Netzsch 404).

For electrical conductivity measurements, gold electrodes were sputtered onto the two circular sides of the glassy samples prior to annealing, using a Quorum QR150 R ES Sputter. Conductivity was determined by impedance spectroscopy in a frequency range of 10 MHz to 5 Hz using a Solartron 1260 Impedance/Gain-Phase Analyzer coupled to a Solartron 1296 Dielectric interface system. The samples were placed in a two-point sample holder and inserted in a Novotherm temperature control furnace, which provides temperature stability of  $\pm 0.1$  K at the sample level. Impedance data were plotted in the complex plane plot, the so-called Nyquist diagram. The resistance ( $R$ ) of the sample is thus obtained from the real axis location of the minimum of the opposite of imaginary part of impedance. Ionic conductivity ( $\sigma$ ) is then calculated using the relation  $\sigma = \frac{1}{R} \frac{l}{S}$  with  $l$  and  $S$  being sample's thickness and area respectively. Using this procedure, conductivity data were continuously collected *in situ* during the structural relaxation process, with over 20 data points per hour.

This *in situ* method ensures more precise results than intermittent measurements, such as density [5] or refractive index [6] as a function

of time. These intermittent methods require samples to be cooled prior to measurement. We argue that this cooling step, which may introduce changes in the property under study, is obviated in the *in situ* method employed here.

In order to analyze samples with different fictive temperatures, one set of  $\text{AgPO}_3$  glass samples was pre-annealed at 433 K (5 K below the  $T_g^{\text{DSC}}$ ) for 24 h, and another set from the same batch, was pre-annealed at 418 K for 50 days. The purpose of this pre-annealing is to allow the glass to reach the structural equilibrium state at these two different temperatures, which will then be the initial glass fictive temperatures,  $T_f(1)$ .

Each glass sample was then inserted in the Novocontrol sample-holder, placed in the furnace, and the isothermal variations in their electrical conductivity were measured at different temperatures during the structural relaxation process of the glass. The furnace reaches the target temperature in less than 10 min. Note that a setup with high precision and high temperature stability is required for these measurements because of the relatively low variations in conductivity during the relaxation process when compared to the Arrhenius temperature dependence of the ionic conductivity of  $\text{AgPO}_3$  glass. Thus, the accuracy of the experimental data is ensured by the thermal stability of the experimental setup ( $\pm 0.1$  K) and by the choice of the impedance spectroscopy technique used for conductivity measurements, eliminating resistance caused by electrode polarization.

The viscosity of  $\text{AgPO}_3$  glass was measured at temperatures close to and below the  $T_g^{\text{DSC}}$  using a homemade penetration viscometer [11]. At a constant temperature, the penetration speed of a metallic rod in the glass enables one to determine the viscosity [12,13]. The penetration rod used here was a 1 mm diameter cylindrical stainless steel needle, and the temperature stability was  $\pm 1$  K.

The conductivity and viscosity were measured in glass samples from the same batch. This was a necessary precaution because  $\text{AgPO}_3$  glasses with the same nominal glass composition but different thermal histories may have different structures [14].

## 3. Results

Fig. 1 shows, as an example, the impedance complex plane plot obtained for the sample equilibrated at 433 K and measured at 428 K. Note that the resistance of the sample, read at the low frequency intercept of the semicircle with the real axis, increases with increasing time, thus the conductivity is decreasing.

Fig. 2 shows the isothermal conductivity variations as a function of time at 413, 418, 423, and 428 K of  $\text{AgPO}_3$  samples pre-annealed

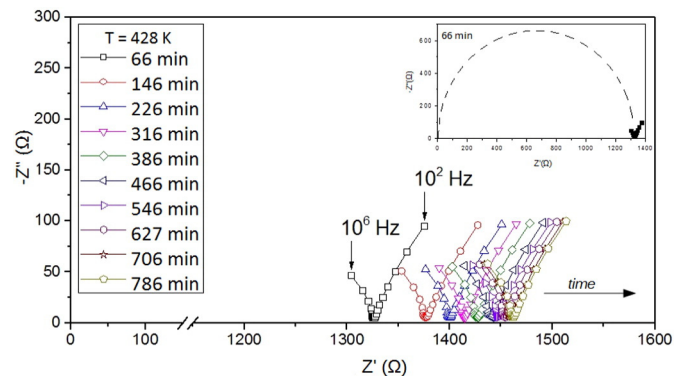
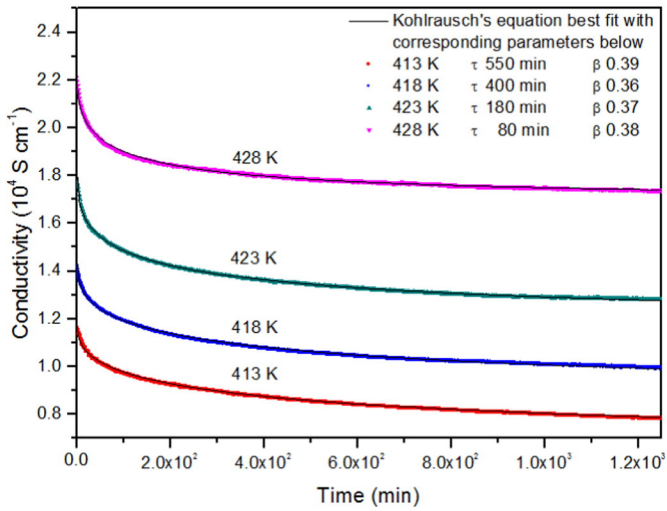
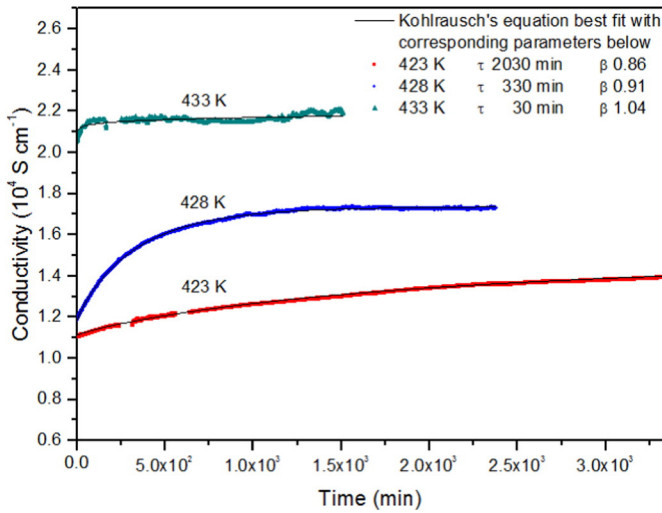


Fig. 1. Evolution with time of the complex plane plot of impedance data for  $\text{AgPO}_3$  glassy sample pre-annealed at 433 K and relaxed at 428 K. Sample's resistance corresponds to the real part of impedance ( $Z'$ ) at the minimum value of the imaginary part ( $-Z''$ ) and increases with time. For clarity, only selected data are shown. Sample's geometrical factor  $l/S = 0.258 \text{ cm}^{-1}$  ( $l$  and  $S$  are, respectively, sample's thickness and area). Lines are guide to the eyes.



**Fig. 2.** Variation of isothermal conductivity as a function of time for  $\text{AgPO}_3$  glass samples pre-annealed at the fictive temperature of 433 K, and then relaxed at different lower temperatures. Full lines correspond to the best fit with the Kohlrausch equation. Note that the experimental data cannot be visually separated from the Kohlrausch fit.



**Fig. 3.** Variation of isothermal conductivity as a function of time for  $\text{AgPO}_3$  glass samples pre-annealed at the fictive temperature of 418 K, and relaxed at different higher temperatures. Full lines correspond to the best fit with the Kohlrausch equation.

at 433 K, while Fig. 3 shows the conductivity variations over time at 423, 428, and 433 K of  $\text{AgPO}_3$  glass samples pre-annealed at 418 K.

**Table 1**

Equilibrium conductivity  $\sigma_\infty$ , characteristic relaxation time  $\tau_\sigma^K$ , average relaxation time  $\langle \tau \rangle$ , and Kohlrausch exponent  $\beta$  (indicated uncertainty is one standard deviation obtained from the non-linear regression), for  $\text{AgPO}_3$  glasses pre-annealed at 433 K or 418 K and subsequently equilibrated at different temperatures. Values are obtained by fitting the data to the Kohlrausch equation (Eq. (4)) using OriginPro 8® software. The coefficient of determination,  $R^2$ , is also indicated.

Pre-annealing temperature ( $T_{f(1)}$ )	Relaxation temperature ( $T_{f(2)}$ )	$\sigma_\infty$ ( $\text{S cm}^{-1}$ )	$\beta$	$\tau_\sigma^K$ (min)	$R^2$	$\langle \tau \rangle$ (min)
433 K	413 K	$1.0 \cdot 10^{-5}$	$0.39 \pm 0.01$	$550 \pm 15$	0.999	$1960 \pm 160$
	418 K	$2.2 \cdot 10^{-5}$	$0.36 \pm 0.01$	$400 \pm 5$	0.998	$1830 \pm 170$
	423 K	$5.2 \cdot 10^{-5}$	$0.37 \pm 0.01$	$180 \pm 3$	0.995	$750 \pm 65$
	428 K	$1.75 \cdot 10^{-4}$	$0.38 \pm 0.01$	$80 \pm 2$	0.996	$310 \pm 30$
418 K	423 K	$1.45 \cdot 10^{-4}$	$0.86 \pm 0.01$	$2030 \pm 9$	0.999	$2190 \pm 20$
	428 K	$1.75 \cdot 10^{-4}$	$0.91 \pm 0.01$	$330 \pm 1$	0.999	$345 \pm 2$
	433 K	$2.15 \cdot 10^{-4}$	$1.07 \pm 0.10$	$30 \pm 1$	0.742	$29 \pm 1$

In both cases, conductivity variations were fitted by the Kohlrausch equation, which is written as:

$$\Phi = \frac{\sigma_t - \sigma_\infty}{\sigma_0 - \sigma_\infty} = \exp \left[ - \left( \frac{t}{\tau_\sigma^K} \right)^\beta \right], \quad (6)$$

where  $\sigma_0$  is the conductivity at time 0,  $\sigma_t$  is the conductivity at a given time  $t$ , and  $\sigma_\infty$  is the equilibrium conductivity at infinite time, which can be estimated by extrapolation. Figs. 2 and 3 also show the Kohlrausch regression (OriginPro® 8). The fitting procedure enables the simultaneous determination of the three adjustable parameters:  $\sigma_\infty$ ,  $\beta$ , and  $\tau_\sigma^K$ , reported in Table 1. It should be noted that, to confirm that the duration of the pre-treatments (24 h at 433 K and 50 days at 418 K) sufficed to relax the samples, measurements were also taken at 433 K and 418 K, respectively, which indicated that no variation occurred in electrical conductivity.

From Figs. 2 and 3 and Table 1 it is clear that both relaxation time  $\tau_\sigma^K$  and the average relaxation time  $\langle \tau \rangle$  strongly decrease with increasing temperature, whether the glass is expanding or contracting, while  $\beta$  has different values when  $T_{f(2)}$  is below or above  $T_{f(1)}$ .

Fig. 4 depicts the isothermal variation in ionic conductivity of both glass samples at 428 K, the first pre-annealed at 433 K and the second at 418 K. In the first case, when the relaxation temperature  $T_{f(2)}$  is below the fictive temperature  $T_{f(1)}$  and therefore, the glass structure contracts, its conductivity decreases over time; in the second case, when the relaxation temperature is above the fictive temperature  $T_{f(1)}$  and the glass structure expands, its conductivity increases over time, both converging to the same value. Similar asymmetrical relaxation curves have been reported from isothermal measurements of viscosity [15–17] and from the variation of density over time [5].

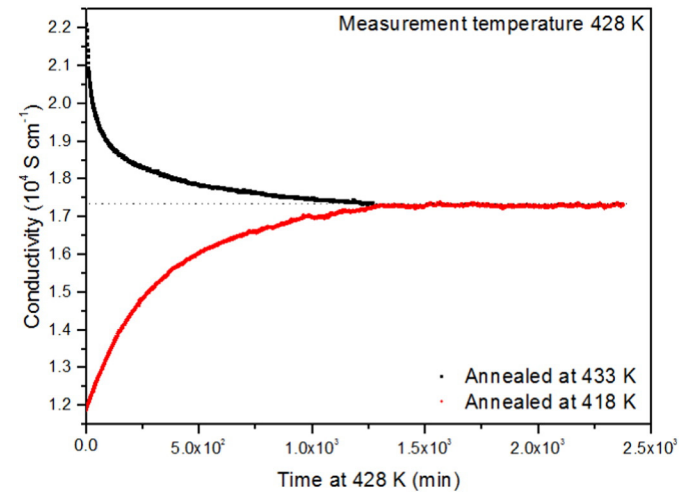


**Fig. 4.** Conductivity variation at 428 K of two  $\text{AgPO}_3$  glassy samples from the same batch annealed, respectively, at 418 K or 433 K, both converging to the same value.

## 4. Discussion

### 4.1. The Kohlrausch exponent

According to the diffusion-trap model postulated by Phillips [18–19], a glass has randomly distributed ‘sinks’ that are able to eradicate neighboring excitations up to a certain distance. During the relaxation process over time, these ‘sinks’ nullify closer excitations, so distant excitations must diffuse over larger distances to reach these sinks. If the excitations are captured by a homogeneous trap density, the capture rate would be constant, leading to a stretch exponent value of  $\beta = 1$ . On the other hand, if the ‘sinks’ are not uniformly distributed, the stretch exponent  $\beta$  would have a different value between 0 and 1.

Phillips expresses the stretching exponent as:

$$\beta = \frac{d^*}{d^* + 2} \quad (7)$$

where  $d^*$  is the effective dimensionality of the channels along which the excitation diffuses.

Potuzak et al. [20] reported two “magic” numbers for  $\beta$  that are different from unity:  $3/5$  and  $3/7$ . The first is associated with the stress relaxation and is obtained from Eq. (7) when the effective dimensionality,  $d^*$ , is equal to three; the second is related to the structural relaxation mechanism governed by long range Coulomb forces, for which  $d^* = 3/2$ .

The glass samples annealed at 433 K and relaxed at lower temperatures, whose structure contracted during relaxation, revealed an average  $\beta$  value of 0.38, which is close to  $3/7$ , suggesting a relaxation mechanism controlled by long range Coulomb forces, as stated above. However, for the glass samples annealed at 418 K and relaxed at higher temperatures, whose structure expanded during relaxation, the average value of  $\beta$  is 0.94, close to 1.

According to Philips, these different  $\beta$  values suggest different microscopic mechanisms for glass contraction and expansion. Following the landscape physics [21,22], when the relaxation process occurs at a temperature  $T_{f(2)}$  lower than the pre-equilibration temperature  $T_{f(1)}$  as shown in Fig. 2, the barriers for structural relaxation are small in the beginning but become larger with increase in time giving rise to a low value of  $\beta$  [21,22], and a low characteristic KWW relaxation time.

On the other hand, when the relaxation occurs at a temperature  $T_{f(2)}$  higher than the equilibration temperature  $T_{f(1)}$  (Fig. 3), initially the barriers are high and mask the effect of lower barriers giving rise to a value of stretching exponent that is closer to unity and a large characteristic KWW-relaxation time. This explains the non-linear relaxation behavior with different values for  $\beta$  and  $\tau$  depending on the initial and final fictive temperatures. Fig. 4 is, thus, another example of the intrinsic non-linear nature of structural relaxation. Changes in the beta values with temperature have also been observed during physical aging of the KKN ionic glass [10].

### 4.2. Viscosity measurements and the Maxwell relationship

From a microscopic standpoint, viscosity is related to the relative rearrangement of a liquid’s constitutive molecules, which, in the present case, are the macromolecular chains of  $(PO_4)^n$  tetrahedra. Above the glass transition temperature, in the supercooled liquid regime, the rearrangement times are shorter than the observational timescale. In this case, equilibrium viscosity is observed.

The chain segments move increasingly slow as the temperature decreases and on a limited observational timescale, equilibrium viscosity is no longer reached. The change from equilibrium to non-equilibrium viscosity leads to a discontinuity [23] along the temperature axis in fragile liquids such as  $AgPO_3$ .

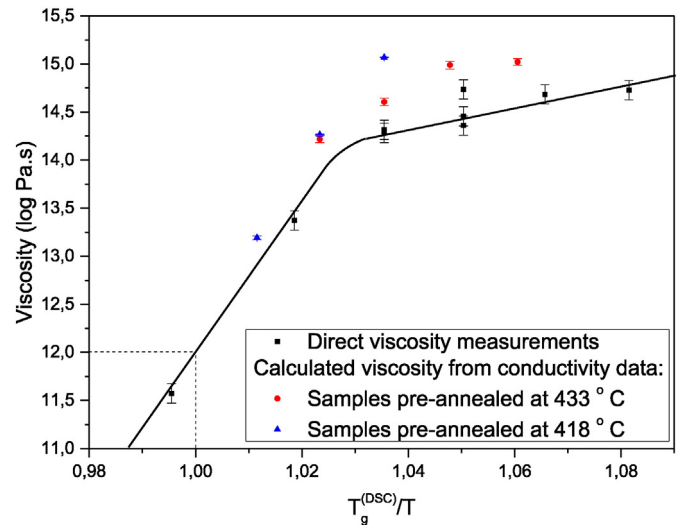


Fig. 5. Experimental viscosity data for  $AgPO_3$  glass obtained by the penetration technique (squares) and calculated by the Maxwell relation  $\eta = G \langle \tau \rangle$ , and values from Table 1, see Section 4.2. Line is a guide to the eye. Error in experimental viscosity was taken as 0.1 in log scale, as suggested by Klyuev [29]. Experimental viscosity data have been scaled to  $10^{12}$  Pa·s at  $T_g^{DSC}$ .

In this work, the timescale of the viscosity measurement is up to two orders of magnitude larger than the DSC timescale. Thus, equilibrium viscosity can be observed below  $T_g^{DSC}$ . The equilibrium and non-equilibrium viscosities are depicted in Fig. 5 by a visible change in slope at  $T_g^{DSC}/T = 1.03$ . A similar behavior of the dependence of viscosity on temperature has been reported for glasses on the  $AgPO_3$ – $AgI$  system [24].

The average structural relaxation time  $\langle \tau \rangle$  previously calculated from conductivity measurements, can be linked to viscosity  $\eta$  by the Maxwell fluid equation,  $\eta = G \langle \tau \rangle$  where  $G$  is the shear modulus at infinite frequency, and  $\langle \tau \rangle$  is defined by Eq. (5).  $G$  is associated with the force constants of chemical bonds [25], and its value ranges from  $3 \cdot 10^9$  to  $30 \cdot 10^9$  Pa in ionic-covalent glasses [26] and from  $0.1 \cdot 10^9$  to  $0.5 \cdot 10^9$  Pa in organic polymers [27]. Fig. 5 shows good agreement between experimental viscosity data and calculated viscosity. The viscosity was calculated using the Maxwell relationship (expression (4)) and the average relaxation time (expression (5)), with  $G = 8.9 \cdot 10^9$  Pa, calculated from the bulk and Young’s modulus of a silver metaphosphate glass, both determined by Brillouin scattering [28]. In expression (5),  $\tau_{\sigma}^K$  and  $\beta$  were obtained from the fitting of conductivity data using the Kohlrausch equation, Figs. 2 and 3.

### 4.3. Fictive temperature and ionic transport

From a microscopic point of view, when the fictive temperature of a supercooled liquid decreases, the energy stored by the deformation of the chemical bonds is released, leading to a decrease in free energy. In the present case, this means that the free energy of the supercooled  $AgPO_3$  follows the same variation as that of the fictive temperature, when it decreases or increases.

According to the weak electrolyte description [30], charge carrier formation would result from a self-dissociation of glassy  $AgPO_3$ , according to the dissociation equilibrium:



to which is associated a dissociation constant  $K$ :

$$K = \frac{[Ag^+][PO_3^-]}{a_{AgPO_3}} \quad \text{or} \quad K = \frac{[Ag^+]^2}{a_{AgPO_3}} \quad (10)$$

in which  $a_{AgPO_3}$  is the thermodynamic activity of silver metaphosphate corresponding to an arbitrary reference state.  $[Ag^+]$  represents the effective charge carrier concentration, probably an interstitial pair, while  $PO_3^-$  is a vacant silver site. These descriptions [31], taken from the point defects model, allow us to describe the formation of a charge carrier in amorphous  $AgPO_3$ .

By definition, the  $AgPO_3$  free energy ( $G_{(AgPO_3)}$ ) is:

$$G_{(AgPO_3)} = G^0_{(AgPO_3)} + RT \ln a_{AgPO_3}. \quad (11)$$

Combining Eqs. (10) and (11) results:

$$[Ag^+] \approx \exp\left(\frac{G_{(AgPO_3)}}{2RT}\right). \quad (12)$$

According to expression (12), at a constant temperature, the concentration in charge carriers  $[Ag^+]$  is an exponential function of the  $AgPO_3$  free energy. A decrease in  $G_{(AgPO_3)}$  caused by a decrease in the fictive temperature will lead to a decrease in the concentration of charge carriers, and consequently, to a decrease in the glass ionic conductivity, and *vice-versa*, as shown in Table 1 and Figs. 2–4.

## 5. Conclusions

In the present work, the kinetics of the structural relaxation time of an ionic conductive glass was analyzed based on *in situ* electrical conductivity measurements.

The advantage of this technique is that it provides isothermal relaxation curves with good statistics, since more than 20 data points per hour can be collected. This is not the case when the relaxation kinetics is determined by measurements of properties such as density or refractive index, which are measured not continuously over time.

The experimental structural relaxation kinetics of silver phosphate glass near and below the DSC glass transition temperature was well described by a Kohlrausch equation, allowing us to determine the characteristic structural relaxation time  $\tau_0^K$  and the stretch exponent,  $\beta$ , for each relaxation curve. Two different values of the stretch exponent were observed: one close to unity as the glass expanded; and the second close to the “magic number” of 3/7 as the glass contracted.

Viscosity was calculated using the Maxwell relation with relaxation times obtained from the Kohlrausch regression of ionic conductivity data and a shear modulus of  $8.9 \cdot 10^9$  Pa taken from the literature. This calculated viscosity is in agreement with the experimental viscosity measured with a penetration viscometer. This agreement is a positive validation of the method used in this paper to estimate structural relaxation time.

## Acknowledgments

The authors gratefully acknowledge the Brazilian Research Funding Agencies CAPES (Federal Agency for the Support and Improvement of Higher Education) (PVE – A005-2013. Process No. 23038.007714/2013-40) and the São Paulo State Research Foundation – FAPESP (CEPID process. N. 2013/07793-6). C. B. Bragatto. is also indebted to the Postgraduate Program in Materials Science and Engineering – PPG-CEM, of UFSCar/DEMa for its financial support. D. R. Cassar gratefully acknowledged The Brazilian National Research Council, CNPq (grant No. 150490/2015–1) J.-L. Souquet. thanks LaMaV for its hospitality while participating in this research work. Edgar D. Zanotto and Prabhat Gupta are deeply acknowledged for their invaluable feedback.

## References

- [1] G.W. Scherer, *Relaxation in Glass and Composite*, Krieger Publishing Company, Malabar, FL, USA, 1992.
- [2] R. Kohlrausch, *Ann. Phys. Chem.* 167 (56) (1854).
- [3] S.V. Nemilov, *Thermodynamic and Kinetic Aspects of the Vitreous State*, CRC Press, Boca Raton, 1995.
- [4] J.P. Malugani, A. Wasniewski, M. Doreau, G. Robert, A.A. Rikabi, *Mater. Res. Bull.* 13 (1978) 427.
- [5] M. Hara, S. Suetoshi, *Rep. Res. Lab.*, 5, Asahi Glass Co Ltd., 1955 126.
- [6] G.W. Scherer, *J. Am. Ceram. Soc.* 67 (1984) 504.
- [7] H.N. Ritland, *J. Am. Ceram. Soc.* 37 (1954) 370.
- [8] M.M. Machado, C.B. Bragatto, A.C.M. Rodrigues, Effect of structural relaxation on the electrical conductivity and density of a window glass, 23rd International Congress of Glass, Book of Abstracts, 2013.
- [9] Z. Wojnarowska, C.M. Roland, K. Kolodziejczyk, A. Swiety-Pospiech, K. Grzybowska, M. Paluch, Quantifying the structural dynamics of pharmaceuticals in the glassy state, *J. Phys. Chem. Lett.* 3 (2012) 1238.
- [10] M. Paluch, Z. Wojnarowska, S. Hensel-Bielowka, *Phys. Rev. Lett.* 110 (2013) 015702.
- [11] O. Peitl, *Comportamento termo-mecânico de borossilicato vítreo* (Master Thesis) Universidade Federal de São Carlos (UFSCar), 1990.
- [12] E.D. Zanotto, *Ceramica* 29 (1982) 135.
- [13] R.W. Douglas, W.L. Armstrong, J.P. Edward, D.A. Hall, *Glass Technol.* 6 (1965) 52.
- [14] P. Grabowski, J.L. Nowinski, K. Kwatek, *J. Non-Cryst. Solids* 415 (2015) 51.
- [15] H.R. Lillie, *J. Am. Ceram. Soc.* 16 (1933) 619.
- [16] A. Sipp, D.R. Neuville, P. Richet, *J. Non-Cryst. Solids* 211 (1997) 281.
- [17] Y. Bottinga, A. Sipp, P. Richet, *J. Non-Cryst. Solids* 290 (2001) 129.
- [18] J.C. Phillips, *J. Stat. Phys.* 77 (1994) 945.
- [19] J.C. Phillips, *Rep. Prog. Phys.* 59 (1996) 1133.
- [20] M. Potuzak, R.C. Welch, J.C. Mauro, *J. Chem. Phys.* 135 (2011) 214502.
- [21] F.H. Stillinger, A topographic view of supercooled liquids and glass formation, *Science* 267 (5206) (1995) 19 (New Series (Mar. 31)).
- [22] P.G. Debenedetti, F.F.H. Stillinger, *Nature* 410 (2001) 259–267.
- [23] O. Mazurin, Y. Startsev, S. Stoljar, *J. Non-Cryst. Solids* 52 (1982) 105.
- [24] H. Kobayashi, H. Takahashi, Y. Hiki, *J. Appl. Phys.* 88 (2000) 3776.
- [25] M.F. Ashby, D.R.H. Jones, M.F. Ashby, *Engineering materials 1: an introduction to their properties and applications*, Butterworth-Heinemann, Oxford, 1996.
- [26] T. Rouxel, *J. Chem. Phys.* 135 (2011) 184501.
- [27] D.W. Van Krevelen, K. Nijenhuis, *Properties of Polymers, Their Correlation With Chemical Structure: Their Numerical Estimation and Prediction From Additive Group Contributions*, Elsevier, Oxford, 2009.
- [28] L. Borjesson, S. Martin, L. Torell, C. Angell, *Solid State Ionics* 18-19 (1986) 431.
- [29] V.P. Klyuev, *Glas. Phys. Chem.* 26 (2000) 559.
- [30] J.-L. Souquet, Ionic transport in glassy electrolytes, in: P.G. Bruce (Ed.), *Solid State Electrochemistry*, Cambridge University Press, Cambridge, 1995.
- [31] A.C.M. Rodrigues, M.L.F. Nascimento, C.B. Bragatto, J.-L. Souquet, *J. Chem. Phys.* 135 (2011) 234504.